Barker, P.F., Camerlenghi, A., Acton, G.D., and Ramsay, A.T.S. (Eds.)
Proceedings of the Ocean Drilling Program, Scientific Results Volume 178

13. Late Miocene to Early Pliocene Radiolarians from Glaciomarine Drift Deposits, ODP Leg 178, Hole 1095B (Bellinghausen Basin, Antarctic Ocean)[1]

David B. Lazarus[2]

ABSTRACT

Early Pliocene to middle late Miocene hemipelagic and distal turbidite sediments from Hole 1095B, near the Antarctic Peninsula, yield moderately abundant, moderately well preserved radiolarian faunas and other biosiliceous material (diatoms, silicoflagellates, and sponge spicules). Preservation characteristics, however, vary strongly even between closely related samples, and there are many intervals of poor preservation. In the 140- to 460-meters below seafloor interval studied, it was possible to identify the following standard Southern Ocean radiolarian zones: Upsilon, Tau, *Amphymenium challengerae, Acrosphaera*? *labrata, Siphonosphaera vesuvius,* and upper *Acrosphaera australis* (total age range ~4–10 Ma). Some normally common radiolarian groups, such as actinommids, are unusually rare in the studied material, and the relative ranges of several individual species, such as *Acrosphaera labrata* vs. *A. australis,* appear to be somewhat anomalous. These observations imply that the ranges of taxa in this section may be somewhat diachronous, due to either local ecologic factors and/or the highly variable preservation of the faunas. Thus, the ages of events reported are probably only approximate, although they are still useful for constraining the age of sediments in this section.

[1]Lazarus, D.B., 2001. Late Miocene to early Pliocene radiolarians from glaciomarine drift deposits, ODP Leg 178, Hole 1095B (Bellinghausen Basin, Antarctic Ocean). *In* Barker, P.F., Camerlenghi, A., Acton, G.D., and Ramsay, A.T.S. (Eds.), *Proc. ODP, Sci. Results,* 178, 1–22 [Online]. Available from World Wide Web: <http://www-odp.tamu.edu/publications/178_SR/VOLUME/CHAPTERS/SR178_13.PDF>. [Cited YYYY-MM-DD]
[2]Museum für Naturkunde, Invalidenstrasse 43, 10115 Berlin, Federal Republic of Germany.
david.Lazarus@rz.hu-berlin.de

Initial receipt: 22 August 2000
Acceptance: 8 May 2001
Web publication: 25 July 2001
Ms 178SR-218

INTRODUCTION AND PREVIOUS WORK

The history of the Antarctic ice sheet, an important component of global climate history, is preserved in sediments of the Southern Ocean. This history can be most directly inferred by examination of sediments near the continent, where glacial and glaciomarine deposits dominate. Dating these sediments, however, has often been very difficult due to generally poor microfossil preservation, reworking, and hiatuses. One of the major goals of Ocean Drilling Program Leg 178 was to recover this glacial record, at least partially, in sediments with sufficient microfossils for good biochronology. For this purpose, several holes were drilled during Leg 178 near the Antarctic Peninsula from fairly deep water deposits at bathyal depths to very shallow water deposits near the coast (Fig. F1).

Antarctic Neogene radiolarian faunas (compared to most other coeval Antarctic planktonic microfossils) are relatively diverse and evolve rapidly but are still not very well known taxonomically—many, perhaps the majority, of species have not yet been described. Despite this taxonomic "deficit," radiolarians are, along with diatoms, the main source of biostratigraphic data in Neogene Southern Ocean sediments. Previous studies have established a zonation scheme that has been applicable throughout the Southern Ocean and that is calibrated by means of paleomagnetics to the standard geologic timescale (Chen, 1975; Lazarus, 1990, 1992; Abelmann, 1990, 1992; Caulet, 1991) (Fig. F2). This zonation is, however, of only moderate resolution, and calibrations are sometimes questionable because of uncertainties in age models used. Calibration is a particular problem in the late Miocene to earliest Pliocene, where hiatuses are unusually common in Southern Ocean records. Recent work by Nishimura et al. (1997) on Holocene material also suggests that in very nearshore regions, full oceanic radiolarian assemblages are not present. Instead, a depauperate assemblage is found that is dominated by species not found in coeval oceanic Southern Ocean assemblages. As previous Neogene biostratigraphic work has been mainly from pelagic sections, it has not been established whether the standard Neogene radiolarian zonation can be applied in nearshore regions as well.

Radiolarians from Leg 178 sites were initially studied by A. Weinheimer (Shipboard Scientific Party, 1999). Because of poor breakdown of samples in the shipboard laboratory, only very general information was obtainable. Her results suggested that reasonably well preserved radiolarians were present in most sites, but older assemblages (early Pliocene and late Miocene) were recovered only in Hole 1095B (Fig. F3). This hole was drilled into a continental rise glaciomarine sediment drift near the Antarctic Peninsula.

The present study reports the late Miocene–earliest Pliocene (~4–10 Ma) radiolarian biostratigraphy from Hole 1095B, with the goals of dating the section for use in Antarctic ice sheet studies; testing the viability of standard zonal schemes in a nonpelagic, relatively nearshore setting; and better calibration of individual events to the paleomagnetic polarity timescale.

MATERIALS

Hole 1095B (66°59.1266'S, 78°29.2699'W; water depth = 3841.6 m) was drilled into the distal flank of an unnamed sediment drift. The sec-

F1. Locations of Leg 178 sites, p. 9.

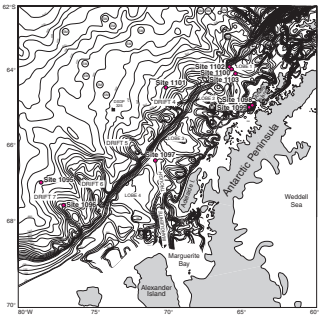

F2. Radiolarian zonation and secondary events, p. 10.

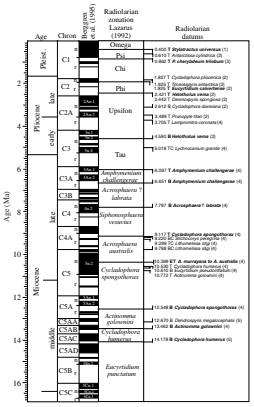

F3. Coring summary and initial biostratigraphic results, p. 11.

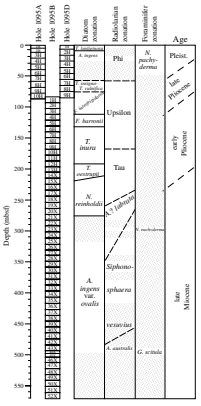

tion was drilled from ~80 to 570 meters below seafloor (mbsf) using the advanced hydraulic piston corer (APC) in the upper 13 cores and the extended core barrel (XCB) for the remainder (Fig. F3). Recovery was generally excellent (average = 79% for the entire hole), although there is a short interval from 214.7 to 233.9 mbsf (Cores 178-1095B-15X and 16X) where recovery was <50%, a gap due to zero recovery in Core 178-1095B-19X at 253.1–262.7 mbsf, and poor recovery in the basal cores of the hole (Cores 178-1095B-43X through 52X). Sediments are mostly diatomaceous silty clays with a complex layered structure caused by the varying influence of distal turbidite and hemipelagic sedimentation (Shipboard Scientific Party, 1999). Shipboard sampling was routinely carried out for radiolarian studies at ~2–4 samples per core. Weinheimer's shipboard study of this hole was based on core catcher samples, which, together with the shipboard age model (Shipboard Scientific Party, 1999), were used to select a subset of samples for detailed analysis from these previously taken samples. In all, 98 samples covering the time interval 4–10 Ma (Cores 178-1095B-5H to 52X) were processed into radiolarian slides (see "Appendix A," p. 17).

METHODS

A "kerosene"-type method was applied for sample preparation. Samples were soaked in a 1% solution of sodium pentametaphosphate, boiled, sieved (these first steps reduced the volume of sample and, thus, the amount of environmentally harmful organic liquid that needed to be used), then dried at ~60°C and soaked while still warm in an liquid organic fuel (in this case grill lighter fluid, as kerosene was not obtainable from our supplier). The liquid was then decanted and sodium pentametaphosphate solution added. Sample breakdown was sometimes quite rapid at this stage. Further processing by repeated cycles of boiling, ultrasound, and sieving were applied as needed to complete breakdown of samples. The >38-µm residues were pipetted onto glass slides, dried, embedded in Canada balsam, and covered with standard (0.17 µm) coverslips. Slides were examined with a Zeiss Axioskop using 100×–600× magnification. A relatively cursory initial survey of all 98 slides was made to check overall abundance of coarse-fraction components and radiolarian faunas. Abundances were estimated semiquantitatively (abundant, common, few, rare, etc., where each major rank corresponds approximately to a factor of four difference in abundance). A low-resolution subset of slides was then examined in detail for biostratigraphy, and additional slides were selected as needed to better constrain individual events. Thus, a total of 33 slides were examined in detail for biostratigraphy, although of these, only 22 had reasonably well preserved radiolarian faunas. Occurrences of selected taxa were noted for each examined slide. Emphasis was given to overall assemblage taxonomic characteristics and to the occurrence of known stratigraphic markers. No attempt is made here to provide a comprehensive survey of the full diversity of the assemblages; only the most common or stratigraphically most significant taxa were recorded. Given the frequently poor preservation and rarity of stratigraphic indicators, semiquantitative abundance data was collected only for samples with (relatively) abundant, well-preserved faunas; for more poorly preserved assemblages or for taxa in noncritical intervals, only presence–absence data was recorded, although it was recorded if the taxon was represented by a single specimen or by more than one specimen. Images of selected

radiolarian specimens were made with a video camera and frame-grabber imaging system (~450 lines of camera resolution) and copied in their original digital form to form the plate figures.

RESULTS

Coarse-Fraction Composition and Radiolarian Abundance

The semiquantitative abundance of radiolarians, diatoms, sponge spicules, silicoflagellates, rock fragments, and amorphous material (clumps of sediment that failed to break down) are shown in Figure F4 and listed in "Appendix A," p. 17. Abundances and variation in abundance of biosiliceous components are both rather high throughout much of the studied interval. Diatoms are the most abundant component, followed by sponge spicules, radiolarians, and silicoflagellates. Radiolarians frequently vary from abundant to rare between adjacent samples with a similar variability, albeit at lower absolute values, for silicoflagellates as well. This degree of variability is unusual in coeval pelagic sediment sections from the Southern Ocean and suggests either rapidly altering local upper-water environmental conditions or frequent episodes of nonbiogenic sediment dilution and lowered preservation during deposition at the seafloor. Diatoms are less variable and usually common to abundant in all samples. This may well be an artifact (recording range limit error) of the pipette method of sample preparation because residue is added to the slide until an optimum slide density is obtained. Diatoms, as the most abundant component in the residue, would, thus, normally be at least common in the large majority of slides made and equally are not allowed to ever be more than the maximum value of "abundant." There is a weakly developed pattern of variation in mean abundances, particularly in the silicoflagellates, at a scale of ~100 m (~1 m.y.), but the pattern and possible correlations between components is not very obvious. Biosiliceous material is essentially absent below Core 178-1095B-46X, to a degree that suggests either substantially different primary upper water environmental conditions or a major change in preservation (pre- or postdepositional).

F4. Coarse-fraction results, p. 12.

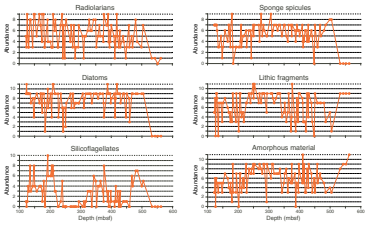

Radiolarian Assemblages

The radiolarian faunas recovered from Hole 1095B (Table T1) are fairly typical pelagic assemblages for this time interval (the full taxonomic list given in "Appendix B," p. 20), with some significant differences. Basal Pliocene and latest Miocene faunas are dominated by *Antarctissa denticulata* and *Antarctissa strelkovi,* which give way in older late Miocene deposits to forms transitional to *Antarctissa deflandrei*. Accessory taxa such as *Cycladophora pliocenica, Prunopyle titan, Lychnocanium grande* (group) in the basal Pliocene to latest Miocene and *Dendrospyris rhodospyroides/haysi, Prunopyle hayesi,* and *Siphonosphaera vesuvius* in older late Miocene samples are also typical. Despite the lack of a full objective treatment of the entire fauna, the general (subjective) impression given by the faunas is of somewhat lower-than-average diversity, even in assemblages with common to abundant individuals and moderate to good preservation. Certain groups, in particular the actinommids and the prunoid/lithelids, seem to be poorly represented in both numbers of taxa and individuals. On the other hand, in at least

T1. Radiolarian range chart, p. 13.

some of the better preserved samples, there is a wealth of plagoniid taxa, although this latter observation may equally reflect the fact that most prior work on Southern Ocean faunas has been done using a 63-µm sieve, which does not retain many of the small plagoniid species.

The less-than-full diversity and somewhat skewed composition at higher taxonomic levels suggest that ecologic restrictions on the distribution of taxa were important in this region in this time interval. The causes are unknown; but in any case, this observation has a significant bearing on the interpretation of the biostratigraphic data.

Biostratigraphy

The studied interval corresponds to the following zones: basal part of the Tau, *Amphymenium challengerae, Amphymenium labrata, S. vesuvius,* and upper *Amphymenium australis* Zones of Lazarus (1992). All zonal markers are seen, and the order of events conforms to expectations (Table T2). However, the relative duration between events, as judged from relative sediment thicknesses, is often rather different than reported by Lazarus (1992) and others. Local ecologic and/or preservational control of event positions may be responsible for this, a suspicion reinforced by the general assemblage characteristics noted above and by the ranges of individual taxa. *A. labrata,* for example, ranges downcore in more open ocean sections to approximately the top of *A. australis* and *S. vesuvius* (e.g., Site 751) (Lazarus, 1992). In Hole 1095B, there is a >100-m gap between these events. It is also possible that the last appearance datum of *A. challengerae* and the last abundant appearance datum of *L. grande* are further upsection than reported here, as the observed tops may be due to the intermittent presence of the taxa within their ranges. Thus, although the section can be assigned standard zonal ages, the accuracy of these age assignments is somewhat questionable.

T2. Radiolarian biostratigraphic events, p. 15.

In addition to the standard marker taxa, several as-yet unnamed taxa were seen within the late Miocene with what appear to be restricted stratigraphic ranges and that are also known to occur in approximately the same time intervals in other Southern Ocean sites (e.g., Sites 745 and 746) (D.B. Lazarus, unpubl. data). Two of these are recorded in Table T1 in this report, are illustrated in Plate P1, and are briefly described in open nomenclature in "Appendix B," p. 20 (specimens from Kerguelen Site 746 were used for illustration because of better preservation of specimens). New taxa such as these may prove to be useful additions to the radiolarian stratigraphy of late Neogene sediments in the Antarctic region.

P1. Prunoid "ringed ellipse" and Antarctissa "bullet," p. 16.

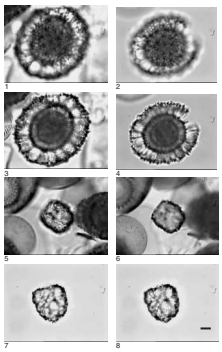

SUMMARY AND CONCLUSIONS

Basal Pliocene and late Miocene sediments from nearshore ODP Hole 1095B contain highly variable amounts of biosiliceous debris, including diatoms, radiolarians, sponge spicules, and silicoflagellates. Radiolarians of typical Antarctic affinities are variably preserved but locally common and abundant in some samples. All previously defined standard zones for this interval (~4–10 Ma) can be identified in the hole between 180 and 460 mbsf, including the basal Tau, *A. challengerae, A. labrata, S. vesuvius,* and upper *A. australis* Zones of Lazarus (1992). Faunas in this relatively nearshore location are, however, unusually deficient in some of the more common taxonomic groups seen in time-equivalent open-ocean pelagic Southern Ocean sections, and the relative ranges of indi-

vidual species are also somewhat different. Thus, although all standard zonal marker events can be identified in the order expected, a degree of diachrony is suspected for at least some of the identified events. The extent to which this affects the accuracy of the age calls cannot be determined except by recourse to independent evidence.

Radiolarian faunas from Hole 1095B provide useful constraints on the age of sediments in the lower part of the hole, but the hole does not appear to be well suited for calibration of radiolarian events, at least for those intended for use in more pelagic sections as well. Additional work on these faunas may yield a more accurately calibrated local zonation scheme, as well as several additional useful biostratigraphic markers from the many as-yet undescribed species in these faunas.

ACKNOWLEDGMENTS

The author wishes to thank Peter Barker and Amy Weinheimer for their invitation to work on this material and for their cooperation throughout the study, Andreas Zingler for sample preparation and generating the coarse-fraction data, and Kjell Bjørklund for a constructive review of the initial manuscript. This work was supported by DFG ODP Schwerpunktprogramm grants LA 1191/1–1 and 1191/1–2.

REFERENCES

Abelmann, A., 1990. Oligocene to middle Miocene radiolarian stratigraphy of southern high latitudes from Leg 113, Sites 689–690, Maud Rise. *In* Barker, P.F., Kennett, J.P., et al., *Proc. ODP, Sci. Results,* 113: College Station, TX (Ocean Drilling Program), 675–708.

————, 1992. Early to middle Miocene radiolarian stratigraphy of the Kerguelen Plateau, Leg 120. *In* Wise, S.W., Jr., Schlich, R., et al., *Proc. ODP, Sci. Results,* 120: College Station, TX (Ocean Drilling Program), 757–783.

Bjørklund, K.R., 1976. Radiolaria from the Norwegian Sea, Leg 38 of the Deep Sea Drilling Project. *In* Talwani, M., Udintsev, G., et al., *Init. Repts. DSDP,* 38: Washington (U.S. Govt. Printing Office), 1101–1168.

Blueford, J., 1982. Miocene actinommid Radiolaria from the equatorial Pacific. *Micropaleontology,* 28:189–213.

Campbell, A.S., and Clark, B.L., 1944. Miocene radiolarian faunas from Southern California. *Spec. Pap.—Geol. Soc. Am.,* 51:1–76.

Caulet, J.-P., 1991. Radiolarians from the Kerguelen Plateau, Leg 119. *In* Barron, J., Larsen, B., et al., *Proc. ODP, Sci. Results,* 119: College Station, TX (Ocean Drilling Program), 513–546.

Chen, P.-H., 1975. Antarctic radiolaria. *In* Hayes, D.E., Frakes, L.A., et al., *Init. Repts. DSDP,* 28: Washington (U.S. Govt. Printing Office), 437–513.

Haeckel, E., 1862. *Die Radiolarien (Rhizopoda Radiolaria):* Berlin (Reimer).

Hays, J.D., 1970. Stratigraphy and evolutionary trends of radiolaria in North Pacific deep sea sediments. *In* Hays, J.D. (Ed.), *Geological Investigations of the North Pacific.* Mem.—Geol. Soc. Am., 126:185–218.

Lazarus, D., 1990. Middle Miocene to Recent radiolarians from the Weddell Sea, Antarctica, ODP Leg 113. *In* Barker, P.F., Kennett, J.P., et al., *Proc. ODP, Sci. Results,* 113: College Station, TX (Ocean Drilling Program), 709–727.

————, 1992. Antarctic Neogene radiolarians from the Kerguelen Plateau, Legs 119 and 120. *In* Wise, S.W., Jr., Schlich, R., et al., *Proc. ODP, Sci. Results,* 120: College Station, TX (Ocean Drilling Program), 785–809.

Lombari, G., and Lazarus, D.B., 1988. Neogene cycladophorid radiolarians from North Atlantic, Antarctic, and North Pacific deep-sea sediments. *Micropaleontology,* 34:97–135.

Martin, G.C., 1904. Radiolaria. *In* Clark, W.B., Eastman, C.R., Glenn, L.C., Bagg, R.M., Bassler, R.S., Boyer, C.S., Case, E.C., and Hollick, C.A. (Eds.), *Systematic Paleontology of the Miocene Deposits of Maryland:* Baltimore (Maryland Geol. Surv., Johns Hopkins Press), 447–459.

Nigrini, C., 1970. Radiolarian assemblages in the North Pacific and their application to a study of Quaternary sediments in core V20-130. *In* Hays, J.D. (Ed.), *Geological Investigations of the North Pacific.* Mem.—Geol. Soc. Am., 126:139–183.

Nigrini, C., and Caulet, J.-P., 1988. The genus *Anthocyrtidium* (Radiolaria) from the tropical late Neogene of the Indian and Pacific Oceans. *Micropaleontology,* 34:341–360.

Nigrini, C., and Moore, T.C., 1979. *A Guide to Modern Radiolaria.* Spec. Publ. Cushman Found. Foraminiferal Res., 16.

Nishimura, A., Nakaseko, K., and Okuda, Y., 1997. A new coastal water radiolarian assemblage recovered from sediment samples from the Antarctic Ocean. *Mar. Micropaleontol.,* 30:29–44.

Petrushevskaya, M.G., 1967. Radiolyarii otryadov Spumellaria i Nassellaria antarkticheskoi oblasti (Antarctic Spumelline and Nasselline radiolarians). In *Resultaty Biologicheskikh Issledovanii Sovetskoi Antarkticheskoi Ekspeditsii 1955–1958* (Vol. 3). Issled. Fauny Morei, Zool. Inst. Akad. Nauk SSSR, 4:1–186.

————, 1975. Cenozoic radiolarians of the Antarctic, Leg 29, DSDP. *In* Kennett, J.P., Houtz, R.E., et al., *Init. Repts. DSDP,* 29: Washington (U.S. Govt. Printing Office), 541–675.

Sanfilippo, A., and Riedel, W.R., 1970. Post-Eocene "closed" theoperid radiolarians. *Micropaleontology,* 16:446–462.

Shipboard Scientific Party, 1999. Site 1095. *In* Barker, P.F., Camerlenghi, A., Acton, G.D., et al., *Proc. ODP, Init. Repts.,* 178 1–174 [CD-ROM]. Available from: Ocean Drilling Program, Texas A&M University, College Station, TX 77845-9547, U.S.A.

Weaver, F.M., 1976. Antarctic Radiolaria from the southeast Pacific basin, Deep Sea Drilling Project, Leg 35. *In* Hollister, C.D., Craddock, C., et al., *Init. Repts. DSDP,* 35: Washington (U.S. Govt. Printing Office), 569–603.

————, 1983. Cenozoic radiolarians from the southwest Atlantic, Falkland Plateau region, Deep Sea Drilling Project Leg 71. *In* Ludwig, W.J., Krasheninnikov, V.A., et al., *Init. Repts. DSDP,* 71 (Pt. 2): Washington (U.S. Govt. Printing Office), 667–686.

Figure F1. Map showing the locations of Site 1095 and other Leg 178 sites (from Shipboard Scientific Party, 1999).

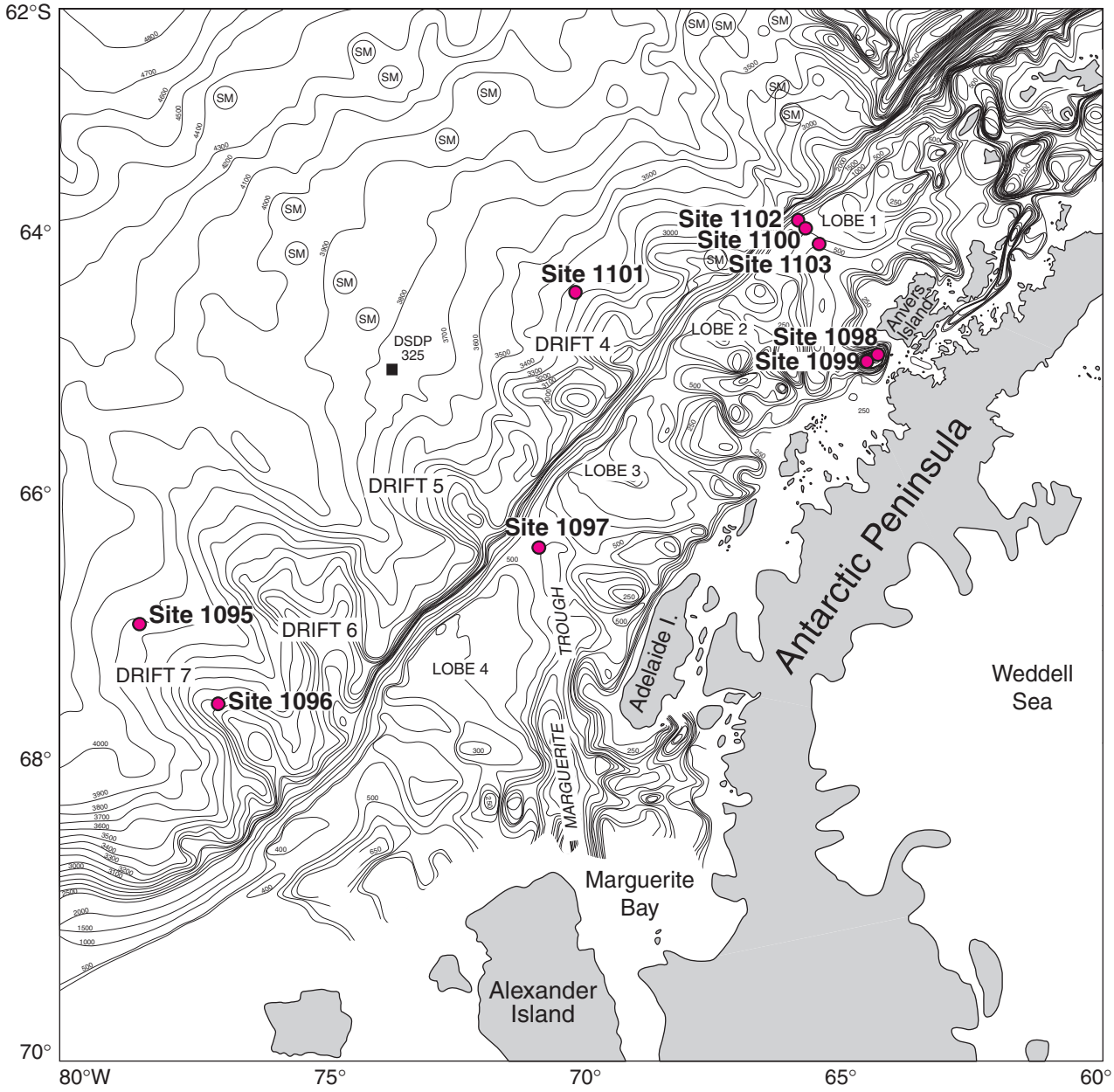

Figure F2. Neogene Southern Ocean radiolarian zonation and secondary events (from compilation by A. Weinheimer, in Shipboard Scientific Party, 1999). T = top, B = bottom, TC = top common, BC = bottom common, ET = evolutionary transition. Events defining full zone boundaries are shown in bold. Numbers in parentheses are the sources of the ages: 1 = Lazarus (1990), 2 = Caulet (1991), 3 = Hays and Opdyke (1967), 4 = Lazarus (1992), 5 = Abelmann (1992).

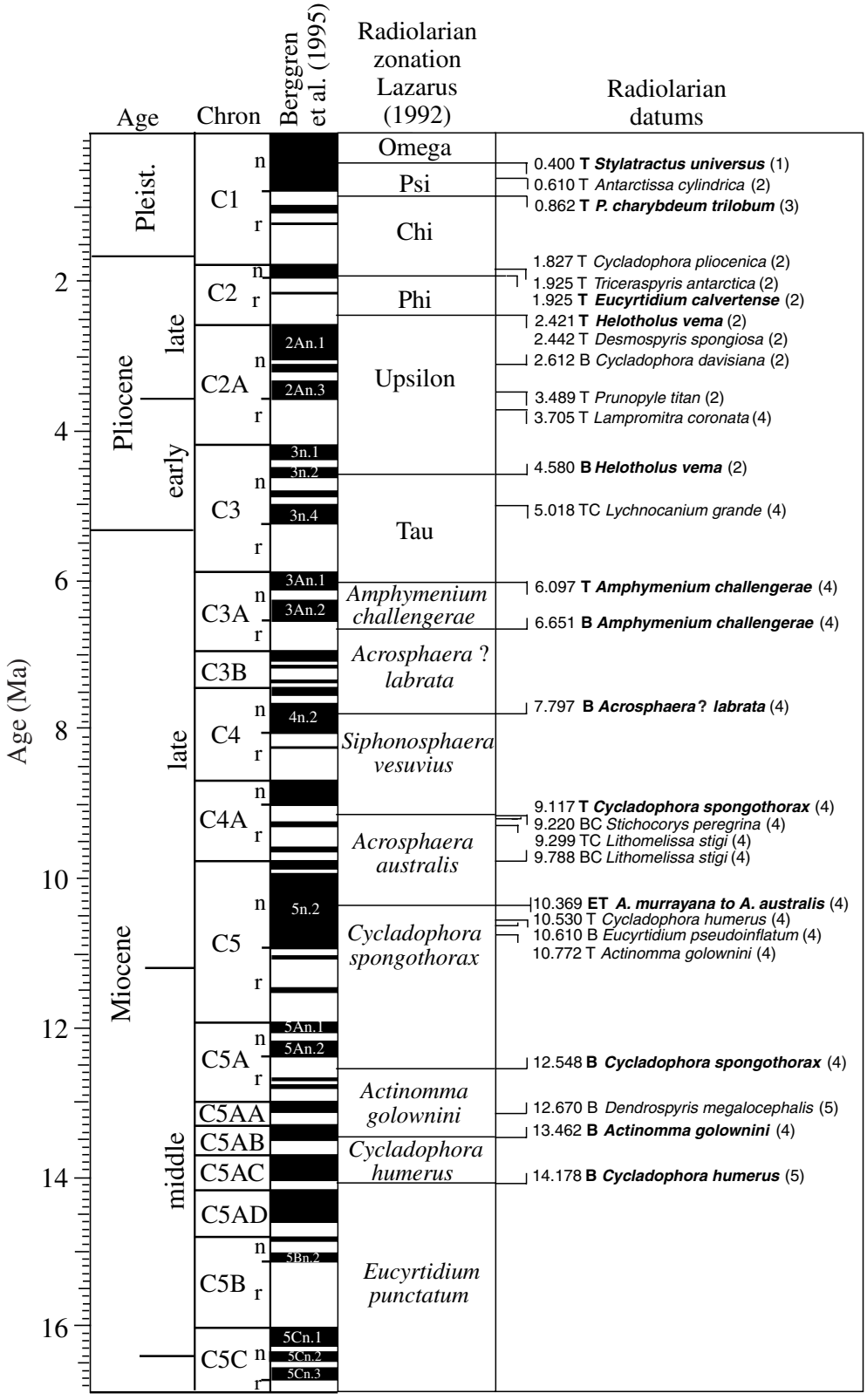

Figure F3. Coring summary and initial shipboard biostratigraphic results, Site 1095 (from Shipboard Scientific Party, 1999).

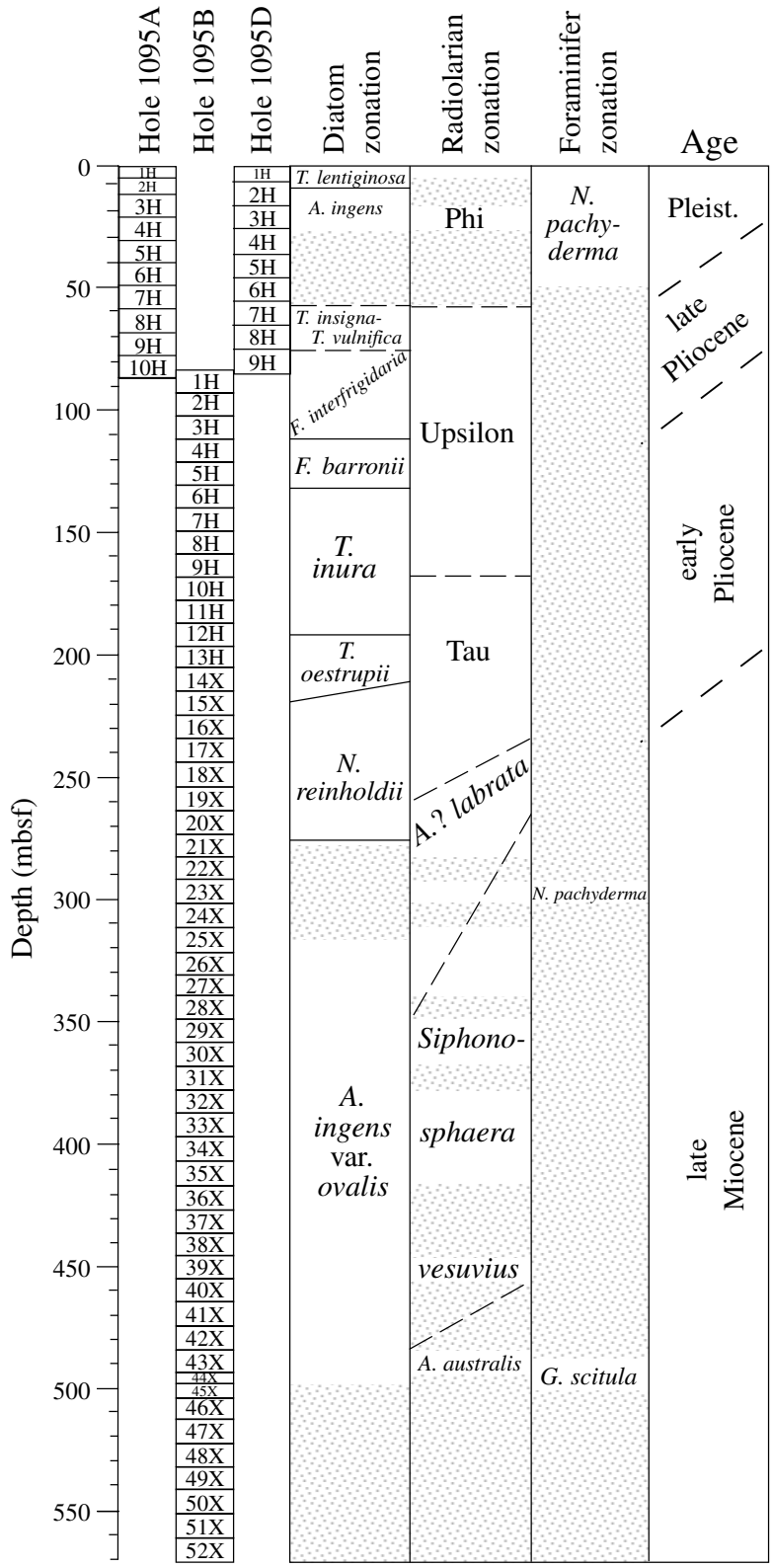

Figure F4. Coarse-fraction results, Hole 1095B. Data is semiquantitative, ranging from very abundant (11) via half-rank steps (e.g., C/A = common to abundant) to barren (0 on scale). A difference of one numerical unit (half-rank step) corresponds to approximately a factor of two difference in abundance. Very abundant means that the majority of all specimens were in this category; very rare (value = 1) refers to just two specimens. Data are given in tabular form in "Appendix A," p. 17.

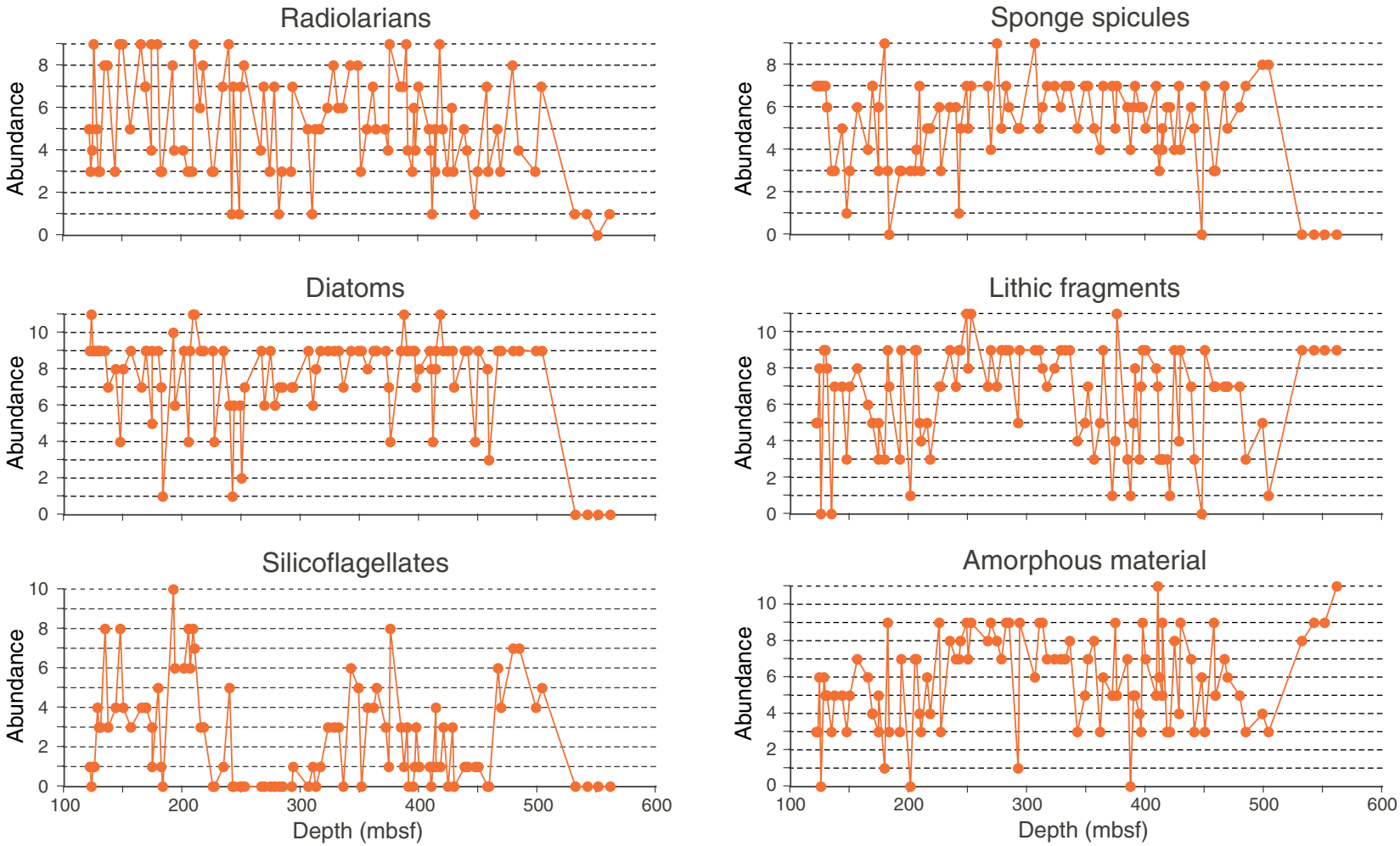

Table T1. Range chart of selected radiolarian taxa, Hole 1095B. (Continued on next page.)

Depth (mbsf):	156.13	165.1	169.62	174.05	174.77	179.37	192.43	201.44	208.47	217.61	227.56	234.29	239.59	243.99	248.85	252.58	266.72	269.49	277.61
Core, section, interval (cm):	8H-5, 63	9H-5, 10-12	10H-1, 112	10H-4, 105	10H-5, 27-29	11H-1, 137-139	12H-4, 43-45	13H-4, 102-104	14X-3, 52-54	15X-2, 141-145	16X-3, 26-28	17X-1, 39-41	17X-4, 119-121	18X-1, 49-51	18X-4, 85-87	18X-7, 8-10	20X-3, 102-104	20X-5, 79-81	21X-4, 71-73
Radiolarian abundance:	F	A	C	R	A	A	C	F/C	R/F	A	R/F	C	A	C/A	R	C/A	R/F	C	C
Radiolarian preservation:	M	M/G	M	M	M	M	G	M	P	M/G	P/M	M/G	G	M/G	P	M	P/M	M	M/G
Lithic fragments:	A	F/C	F		C/A	R	R	R	F	F/C	F	A	A	A	VA	VA		VA	VA
Centric diatoms:	A	C	A		C/A	F	A	A	VA	C	F	A	C	C	C	C/A		F	C
Pennate diatoms:	C	C	C/A		CA	A	A	C	F	F	R	C	F	F		C		R	R
Sponge spicules:	C/A	F	C		C	F	R	R	C	F	F	C		C	C	C/A		C	C
Silicoflagellates:	F		F			F	VA	F/C	A	R/F	R								
Stylatractus sp. cf. *universus*							X			R	X			X					F/C
Druppatractus hastatus										R				X					X
Prunopyle titan		R/F	X	X	C	X				R			X	?		X		?	
Prunopyle hayesi																			
Prunoid "elliptical rings"																X		X	X
Amphymenium challengerae										–		–	R/F	R		VR			
Siphonosphaera vesuvius	+																		
Acrosphaera labrata										F		X	F/C	R/F		C			
Acrosphaera australis																			
Acrosphaera? *mercurius*					R	X	X	X	X	X	X		X	X		X			
Triceraspyris coronata group				X?	C/A	X				F/C									
Desmospyris spongiosa	F?	C	X	+?															
Dendrospyris rhodospyroides						?													
Dendrospyris haysi										R						X			
Lychnocanium grande group		R/F	+		R/F					F/C	X	X	F	C		X		F	X
Stichocorys sp. cf. *peregrina*																			X
Anthocyrtidium sp. cf. *ehrenbergi*																			
Eucyrtidium pseudoinflatum		R	X		R/F					F/C			X	X		X			X
Eucyrtidium calvertense					R/F	X	X					X		X					?
Lithomelissa stigi																			
Helotholus haysi														R					
Helotholus vema		R?	X	+?															
Antarctissa strelkovi		A	X	X	A	X	X	X	X	F		X	A	X		X		X	X
Antarctissa denticulata						X	X	X	X	F/C		X	X	X				X	X
Antarctissa deflandrei																			
Antarctissa cylindrica		F			R	X		X											
Antarctissa "bullet"									X					X		X			
Lampromitra coronata			X				X		X	+				X					?
Cycladophora spongothorax																			
Cycladophora pliocenica	+	F	X		F/C	X	X	X	X	F				X		X			X
Cycladophora bicornis											X	X		X				X	X

Note: Shaded columns indicate samples with relatively poor preservation. X = presence, blank cell = not observed, – = absence specifically checked for, + = single specimen, ? = questionable identification. Abundance: VA = very abundant, A = abundant, C/A = common to abundant, C = common, F/C = few to common, F = few, R/F = rare to few, R = Rare, and VR = very rare. Data are semiquantitative; each half-rank step corresponds to approximately a factor of two difference in abundance. Very abundant means that the majority of all specimens were in this category; very rare refers to just two specimens.

Table T1 (continued).

Depth (mbsf):	284.45	293.98	3.9.81	317.1	323.02	332.38	342.72	351.75	364.2	374.33	385.18	399.37	409.04	410.09	411.38	413.55	420.52	440.51	466.6
Core, section, interval (cm):	22X-2, 85-87	23X-2, 78-80	24X-6, 101-103	25X-5, 20-22	26X-2, 92-4	27X-2, 68-69	28X-2, 142-143	29X-2, 76-77	30X-4, 50-52	31X-4, 103-105	32X-5, 78-80	34X-2, 57-58	35X-2, 94-96	35X-3, 49-51	35X-4, 28-30	35X-5, 36-37	36X-3, 132-134	38X-4, 51-53	41X-2, 60-62
Radiolarian abundance	R	F/C	VR	R/F	C/A	C	C	R	C	F/C	C	C/A	R/F	R	R	F/C	C	F	F/C
Radiolarian preservation	M	M	P	P/M	M	M/G	G	P/M	M/G	P/M	M	M	P/M			M	M	P/M	M
Lithic fragments	VA	VA	A	A	A	C/A	F	A	C	F/C	F	VA	A			F	F	F	C
Centric diatoms	C	C	A	A	VA	VA	A	A	VA	A	VA	A	VA			A	A	A	A
Pennate diatoms	R	R	-	R		R	F/C	R	C	F	C	F	C			A	A	A	C
Sponge spicules	C{A	C/A	C/A	A	A	C/A	F/C	A	C	C	C	C/A	C			C	F	C	C
Silicoflagellates	-	R	R	R/F	F	F	F	R	F	R/F	R	R	R			R/F	R	R	F
Stylatractus sp. cf. *universus*		X					R/F		X								X		
Druppatractus hastatus	X				C	X	X		X		+						X		
Prunopyle titan							X					X					R		
Prunopyle hayesi												+				X	R/F		X
Prunoid "elliptical rings"					X		C		X		R	X							
Amphymenium challengerae																			
Siphonosphaera vesuvius									R/F	X	F	X	X			X	F/C	F	X
Acrosphaera labrata																			
Acrosphaera australis									R/F	X	F	X	X				VR		X
Acrosphaera? mercurius							X					X							
Triceraspyris coronata group		X			VR														
Desmospyris spongiosa																			
Dendrospyris rhodospyroides											?	?				?		?	?
Dendrospyris haysi												X				?	X		?
Lychnocanium grande group	X	C	?		R		X				R	X							
Stichocorys sp. cf. *peregrina*	X	F/C			VR		F/C										VR		
Anthocyrtidium sp. cf. *ehrenbergi*		X										X							
Eucyrtidium pseudoinflatum							X		X		X	X					R		
Eucyrtidium calvertense												X							
Lithomelissa stigi					+		?				R								
Helotholus haysi												?	X				R	VR	X
Helotholus vema																			
Antarctissa strelkovi		X			F	X	F		X	?	A	?				X	?	X	
Antarctissa denticulata	X	X			F/C		A	X	X	?	C	X	X			?	X		X
Antarctissa deflandrei										?		?				?	?	X	X
Antarctissa cylindrica																			
Antarctissa "bullet"	?				C	?	F/C	R	X	X	C	X	X			VR	C/A	-	
Lampromitra coronata						X					R	X	X				X		
Cycladophora spongothorax									?							R	R/F	R	X
Cycladophora pliocenica																			
Cycladophora bicornis		X			F	X	X		X		R	X	X			X		R	X

Table T2. Radiolarian biostratigraphic events, Hole 1095B.

Event	Top core, section interval (cm)	Bottom core, section, interval (cm)	Age (Ma)
	178-1095B-	178-1095B-	
FAD *H. vema*	10-1, 112	10-5, 27	4.6
FAD *D. spongiosa*	10-1, 112	10-5, 27	4.6
LAAD *L. grande*	14-3, 52	15-2, 141	5.0
LAD *A. challengerae*	17-1, 39	17-4, 119	6.1
FAD *A. challengerae*	18-7, 8	20-5, 79	6.6
FAD *A. ? labrata*	20-5, 79	21-4, 71	7.8
LAD *C. spongothorax*	34-2, 57	35-5, 36	9.1

Notes: LAD = Last appearance datum, FAD = first appearance datum, LAAD = last abundant appearance datum.

Plate P1. 1–4. Prunoid "ringed ellipse" (Sample 119-746A-5H-1, 53 cm). **5–8.** *Antarctissa* "bullet." (5, 6) Sample 119-746A-6H-3, 53 cm; (7, 8) Sample 119-746A-7H-6, 53 cm. For each of the four illustrated specimens, two views at different focal depths are shown. Scale bar is in the lower right corner for all figures; scale bar = 20 µm. All specimens are from Kerguelen Plateau Site 746.

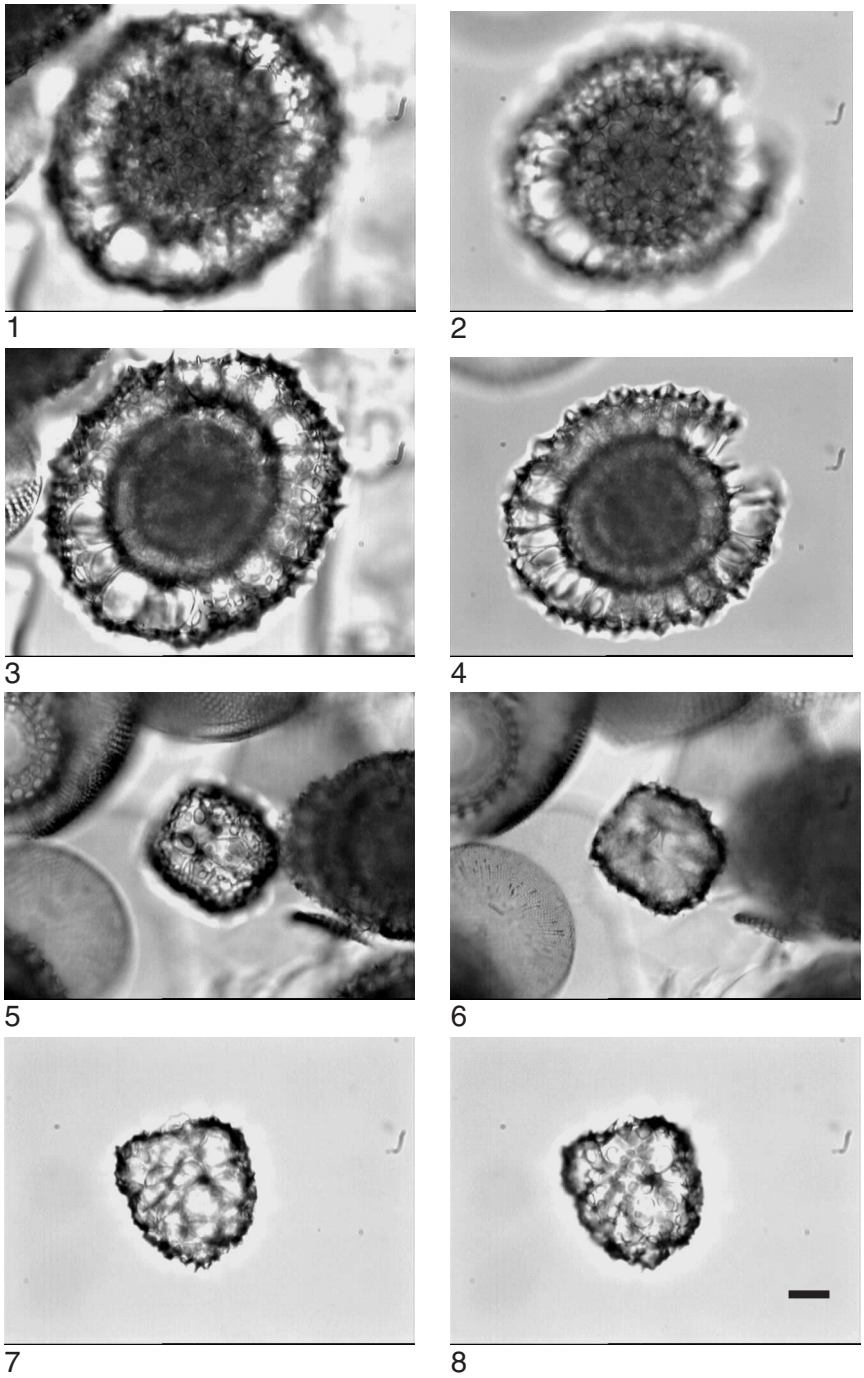

APPENDIX A

Sample List and Coarse-Fraction Values

Core, section, interval (cm)	Depth (mbsf)	Radiolarians (abundance)	Depth (mbsf)	Diatoms (abundance)	Depth (mbsf)	Silicoflagellates (abundance)	Depth (mbsf)	Spicules (abundance)	Depth (mbsf)	Lithic fragments (abundance)	Depth (mbsf)	Amorphous sediment (abundance)
178-1095B-												
5H-1, 137-139	122.37	5	122.37	9	122.37	1	122.37	7	122.37	5	122.37	3
5H-2, 57-59	123.07	3	123.07	11	123.07	0	123.07	7	123.07	5	123.07	3
5H-3, 13-15	124.13	4	124.13	9	124.13	1	124.13	7	124.13	8	124.13	6
5H-4, 23-25	125.73	9	125.73	9	125.73	1	125.73	7	125.73	0	125.73	0
5H-5, 98-100	127.98	5	127.98	9	127.98	4	127.98	7	127.98	9	127.98	6
5H-6, 67-69	129.17	3	129.17	9	129.17	3	129.17	7	129.17	9	129.17	5
5H-7, 52-54	130.52	3	130.52	9	130.52	3	130.52	6	130.52	8	130.52	5
6H-4, 23-25	135.23	8	135.23	9	135.23	8	135.23	3	135.23	0	135.23	3
6H-5, 80-82	137.3	8	137.3	7	137.3	3	137.3	3	137.3	7	137.3	5
7H-3, 105-107	144.02	3	144.02	8	144.02	4	144.02	5	144.02	7	144.02	5
7H-6, 50-52	147.97	9	147.97	4	147.97	8	147.97	1	147.97	3	147.97	3
8H-1, 79-81	150.29	9	150.29	8	150.29	4	150.29	3	150.29	7	150.29	5
8H-5, 63-65	156.13	5	156.13	9	156.13	3	156.13	6	156.13	8	156.13	7
9H-5, 10-12	165.1	9	165.1	7	165.1	4	165.1	4	165.1	6	165.1	6
10H-1, 112-114	169.62	7	169.62	9	169.62	4	169.62	7	169.62	5	169.62	4
10H-1, 112-114	169.62	7	169.62	9	169.62	4	169.62	7	169.62	5	169.62	4
10H-4, 105-107	174.05	4	174.05	5	174.05	3	174.05	3	174.05	3	174.05	3
10H-5, 27-29	174.77	9	174.77	9	174.77	1	174.77	6	174.77	5	174.77	5
11H-1, 137-139	179.37	9	179.37	9	179.37	5	179.37	9	179.37	3	179.37	1
11H-3, 126-128	182.26	3	182.26	7	182.26	1	182.26	3	182.26	9	182.26	9
11H-4, 51-53	183.01	3	183.01	1	183.01	0	183.01	0	183.01	7	183.01	3
12H-4, 43-45	192.43	8	192.43	10	192.43	10	192.43	3	192.43	3	192.43	3
12H-5, 12-14	193.62	4	193.62	6	193.62	6	193.62	3	193.62	9	193.62	7
13H-4, 102-104	201.44	4	201.44	9	201.44	6	201.44	3	201.44	1	201.44	0
14X-1, 25-27	205.25	3	205.25	4	205.25	8	205.25	3	205.25	9	205.25	7
14X-2, 19-21	206.64	3	206.64	9	206.64	6	206.64	4	206.64	9	206.64	7
14X-3, 52-54	208.47	3	208.47	11	208.47	8	208.47	7	208.47	5	208.47	4
14X-4, 113-115	210.58	9	210.58	11	210.58	7	210.58	3	210.58	4	210.58	3
15X-1, 73-75	215.43	6	215.43	9	215.43	3	215.43	5	215.43	5	215.43	6
15X-2, 141-143	217.61	8	217.61	9	217.61	3	217.61	5	217.61	3	217.61	4
16X-2, 33-35	226.13	3	226.13	9	226.13	0	226.13	6	226.13	7	226.13	9
16X-3, 26-28	227.56	3	227.56	4	227.56	0	227.56	3	227.56	7	227.56	3
17X-1, 39-41	234.29	7	234.29	9	234.29	1	234.29	6	234.29	9	234.29	8
17X-4, 119-121	239.59	9	239.59	6	239.59	5	239.59	6	239.59	7	239.59	7
17X-6, 126-128	242.66	1	242.66	1	242.66	0	242.66	1	242.66	9	242.66	7
18X-1, 49-51	243.99	7	243.99	6	243.99	0	243.99	5	243.99	9	243.99	8
18X-4, 85-87	248.85	1	248.85	6	248.85	0	248.85	7	248.85	11	248.85	9
18X-5, 62-64	250.12	7	250.12	2	250.12	0	250.12	5	250.12	8	250.12	7
18X-7, 8-10	252.58	8	252.58	7	252.58	0	252.58	7	252.58	11	252.58	9
20X-3, 102-104	266.72	4	266.72	9	266.72	0	266.72	7	266.72	7	266.72	8
20X-5, 79-81	269.49	7	269.49	6	269.49	0	269.49	4	269.49	9	269.49	9
21X-2, 52-54	274.42	3	274.42	9	274.42	0	274.42	9	274.42	7	274.42	8
21X-4, 71-73	277.61	7	277.61	6	277.61	0	277.61	5	277.61	9	277.61	7
22X-1, 26-28	282.36	1	282.36	7	282.36	0	282.36	7	282.36	9	282.36	9

APPENDIX A (continued).

Core, section, interval (cm)	Depth (mbsf)	Radiolarians (abundance)	Depth (mbsf)	Diatoms (abundance)	Depth (mbsf)	Silicoflagellates (abundance)	Depth (mbsf)	Spicules (abundance)	Depth (mbsf)	Lithic fragments (abundance)	Depth (mbsf)	Amorphous sediment (abundance)
22X-2, 85-87	284.45	3	284.45	7	284.45	0	284.45	6	284.45	9	284.45	9
23X-1, 97-99	292.67	3	292.67	7	292.67	0	292.67	5	292.67	5	292.67	1
23X-2, 78-80	293.98	7	293.98	7	293.98	1	293.98	5	293.98	9	293.98	9
24X-4, 27-29	306.07	5	306.07	9	306.07	0	306.07	9	306.07	9	306.07	6
24X-6, 101-103	309.81	1	309.81	6	309.81	1	309.81	5	309.81	9	309.81	9
25X-2, 55-57	312.95	5	312.95	8	312.95	0	312.95	6	312.95	8	312.95	9
25X-5, 20X-22	317.1	5	317.1	9	317.1	1	317.1	7	317.1	7	317.1	7
26X-2, 92-94	323.02	6	323.02	9	323.02	3	323.02	7	323.02	8	323.02	7
26X-6, 54-56	328.64	8	328.64	9	328.64	3	328.64	6	328.64	9	328.64	7
27X-2, 68-69	332.38	6	332.38	9	332.38	3	332.38	7	332.38	9	332.38	7
27X-4, 86-87	335.56	6	335.56	7	335.56	0	335.56	7	335.56	9	335.56	8
28X-2, 142-143	342.72	8	342.72	9	342.72	6	342.72	5	342.72	4	342.72	3
28X-7, 30-31	349.1	8	349.1	9	349.1	5	349.1	7	349.1	5	349.1	5
29X-2, 75-77	351.75	3	351.75	9	351.75	0	351.75	7	351.75	7	351.75	7
29X-5, 75-77	356.25	5	356.25	8	356.25	4	356.25	5	356.25	3	356.25	8
30X-2, 141-143	362.11	7	362.11	9	362.11	4	362.11	4	362.11	5	362.11	3
30X-4, 50-52	364.2	5	364.2	9	364.2	5	364.2	7	364.2	9	364.2	6
31X-2, 117X-119	371.47	5	371.47	9	371.47	3	371.47	7	371.47	1	371.47	5
31X-4, 103-105	374.33	4	374.33	7	374.33	1	374.33	5	374.33	4	374.33	9
31X-5, 139-141	376.19	9	376.19	4	376.19	8	376.19	7	376.19	11	376.19	5
32X-5, 78-80	385.18	7	385.18	9	385.18	3	385.18	6	385.18	3	385.18	7
32X-6, 145-147	387.35	7	387.35	11	387.35	1	387.35	4	387.35	1	387.35	0
33X-2, 116X-118	390.36	9	390.36	9	390.36	3	390.36	6	390.36	5	390.36	5
33X-3, 91-93	391.61	4	391.61	9	391.61	0	391.61	7	391.61	8	391.61	5
33X-5, 69-71	394.39	3	394.39	9	394.39	0	394.39	6	394.39	3	394.39	4
33X-6, 40-42	395.6	6	395.6	9	395.6	1	395.6	6	395.6	7	395.6	3
33X-7, 13-15	396.83	4	396.83	7	396.83	3	396.83	6	396.83	9	396.83	9
34X-2, 57-58	399.37	7	399.37	8	399.37	1	399.37	5	399.37	9	399.37	7
35X-2, 94-96	409.04	5	409.04	9	409.04	1	409.04	7	409.04	8	409.04	5
35X-3, 49-51	410.09	4	410.09	8	410.09	0	410.09	4	410.09	7	410.09	11
35X-4, 28-30	411.38	1	411.38	4	411.38	1	411.38	3	411.38	3	411.38	6
35X-5, 95-97	413.55	5	413.55	8	413.55	4	413.55	5	413.55	3	413.55	5
35X-6, 51-53	414.61	3	414.61	9	414.61	1	414.61	4	414.61	3	414.61	9
36X-1, 124-126	417.44	9	417.44	11	417.44	1	417.44	6	417.44	3	417.44	3
36X-3, 132-134	420.52	5	420.52	9	420.52	3	420.52	6	420.52	1	420.52	3
36X-6, 5052	424.2	3	424.2	9	424.2	0	424.2	4	424.2	9	424.2	8
37X-2, 80-82	428.1	6	428.1	9	428.1	3	428.1	7	428.1	4	428.1	4
37X-3, 45-47	429.25	3	429.25	7	429.25	0	429.25	4	429.25	9	429.25	9
38X-2, 120X-122	438.2	5	438.2	9	438.2	1	438.2	6	438.2	7	438.2	7
38X-4, 51-53	440.51	4	440.51	9	440.51	1	440.51	5	440.51	3	440.51	3
39X-2, 45-46	447.05	1	447.05	4	447.05	1	447.05	0	447.05	0	447.05	6
39X-4, 62-63	450.22	3	450.22	9	450.22	1	450.22	7	450.22	9	450.22	3
40X-2, 100-102	457.3	7	457.3	8	457.3	0	457.3	3	457.3	7	457.3	9
40X-4, 29-31	459.59	3	459.59	3	459.59	0	459.59	3	459.59	7	459.59	5
41X-2, 60-62	466.6	5	466.6	9	466.6	6	466.6	7	466.6	7	466.6	7
41X-4, 25-27	469.25	3	469.25	9	469.25	4	469.25	5	469.25	7	469.25	6
42X-4, 63-64	479.23	8	479.23	9	479.23	7	479.23	6	479.23	7	479.23	5
43X-1, 60-61	484.4	4	484.4	9	484.4	7	484.4	7	484.4	3	484.4	3
45X-2, 23-25	499.23	3	499.23	9	499.23	4	499.23	8	499.23	5	499.23	4
46X-1, 71-72	503.71	7	503.71	9	503.71	5	503.71	8	503.71	1	503.71	3

APPENDIX A (continued).

Core, section, interval (cm)	Depth (mbsf)	Radiolarians (abundance)	Depth (mbsf)	Diatoms (abundance)	Depth (mbsf)	Silicoflagellates (abundance)	Depth (mbsf)	Spicules (abundance)	Depth (mbsf)	Lithic fragments (abundance)	Depth (mbsf)	Amorphous sediment (abundance)
49X-1, 45-46	532.55	1	532.55	0	532.55	0	532.55	0	532.55	9	532.55	8
50X-1, 79-81	542.49	1	542.49	0	542.49	0	542.49	0	542.49	9	542.49	9
51X-1, 25-27	551.65	0	551.65	0	551.65	0	551.65	0	551.65	9	551.65	9
52X-1, 20X-22	561	1	561	0	561	0	561	0	561	9	561	11

APPENDIX B

Taxonomic List

Citations and/or descriptions for all taxa listed here are given in Lazarus (1992), with the exceptions noted individually below.

Order Spumellaria Ehrenberg, 1875.

Collosphaeridae Müller, 1858.

Acrosphaera Haeckel, 1881.

Acrosphaera australis, Lazarus, 1990, pp. 712–713 (pl. 1, figs. 1–6).

Acrosphaera? labrata, Lazarus, 1992, pp. 793–794 (pl. 1, figs. 1–10).
Remarks: Forms seen are comparatively "late forms" with reduced bar widths and resemble to some degree the shell structure of an orosphaerid.

Acrosphaera? *mercurius,* Lazarus, 1992, p. 794 (pl. 1, figs. 11–16).

Siphonosphaera, Müller, 1858.

Siphonosphaera vesuvius, Lazarus, 1992, pp. 794–795 (pl. 2, figs. 1–8).

Actinommidae Haeckel, 1862, emend. Sanfilippo and Riedel, 1980.

Stylatractus Haeckel, 1887.

Stylatractus universus Hays, 1970, p. 215 (pl. 1, fig. 1); Lazarus, 1990, p. 717 (pl. 6, figs. 9–11).

Amphistylus Haeckel, 1881.

Amphistylus angelinus (Campbell and Clark) Chen, 1975, p. 453 (pl. 21, figs. 3, 4).
Remarks: In Lazarus (1992), the above two species were noted to be similar and were thought to represent an evolutionary lineage *A. angelinus* > *S. universus,* with the transition occurring in the middle Miocene. The forms seen here in the late Miocene and recorded under the name *S.* sp. cf. *universus* appear to be intermediate between *S. universus* and *A. angelinus.*

Druppatractus Haeckel, 1887.

Druppatractus hastatus Blueford, 1982, pp. 206–208 (pl. 6, figs. 3, 4).

Saturnalis Haeckel, 1881.

Saturnalis circularis Haeckel, 1887, p. 131; Chen, 1975, p. 454 (pl. 24, fig. 2).

Spongodiscidae Haeckel, 1862, emend. Riedel, 1967.

Amphymenium Haeckel, 1881.

Amphymenium challengerae Weaver, 1983, p. 675 (pl. 6, figs. 1, 2).

Spongotrochus Haeckel, 1860.

Spongotrochus glacialis Popofsky, 1908; Nigrini and Moore, 1979, p. S117 (pl. 15, fig. 2a–2d).

Pyloniidae Haeckel, 1881.

Prunopyle Dreyer, 1889.

Prunopyle titan Campbell and Clark, 1944, p. 20 (pl. 3, figs. 1–3); Lazarus, 1990, p. 717 (pl. 5, figs. 1–4).

Prunopyle hayesi Chen, 1975, p. 454 (pl. 9, figs. 3–5); Lazarus, 1990, p. 717 (pl. 5, figs. 5–8).

Prunopyle sp. "elliptical rings" (Pl. **P1,** figs. 1–4).

Remarks: The medium-large prunoid species is characterized by four to five elliptical shells, the outermost with clear larcoid gaps at the acute polar ends. Shell wall characteristics are similar to *Lithelius nautiloides*—fairly coarse, rounded pore and bar structure with rough, thorny surface. Shells are connected by numerous fairly stout radial beams. These are few–common in many late Miocene Antarctic samples, including Sites 745 and 746 on the Kerguelen Plateau.

Order Nassellaria Ehrenberg, 1875.

Suborder Spyrida Ehrenberg, 1847, emend. Petrushevskaya, 1971.

Desmospyris Haeckel, 1881.

Desmospyris rhodospyroides Petrushevskaya, 1975, p. 593 (pl. 10, figs. 27–29, 31, 32); Lazarus, 1992, p. 797 (pl. 7, fig. 4).

Dendrospyris "haysi" Lazarus, 1992, p. 797 (pl. 7, fig. 4).

Remarks: *D. "haysi"* in this report refers to the relatively fine-pored variant of *D. rhodospyroides*. It is not clear if this is really a distinct species or what the precise morphologic boundary between the two forms should be, but the *D."haysi"* form seems more characteristic for the late Miocene and the more robust *D. rhodospyroides* form for the older Miocene; thus, they were recorded separately here.

Triceraspyris Haeckel, 1881.

Triceraspyris coronata Weaver, 1976, p. 580 (pl. 2, figs. 4–5; pl. 6, figs. 8–9), Lazarus, 1992, p. 797 (pl. 7, figs. 5–9).

Plagoniidae Haeckel, 1881, emend. Riedel, 1967.

Antarctissa Petrushevskaya, 1967.

Antarctissa deflandrei (Petrushevskaya) Lazarus, 1990, p. 713 (pl. 3, figs. 18, 19).

Antarctissa denticulata (Ehrenberg) Petrushevskaya, 1967, pp. 84–86 (fig. 49, I–IV); Lazarus, 1990, pp. 713–714 (pl. 3, figs. 1–4).

Antarctissa strelkovi Petrushevskaya, 1967, p. 89 (pl. 51, figs. 3–6); Lazarus, 1990, pp. 713–715 (pl. 3, figs. 13–15).

Antarctissa cylindrica Petrushevskaya, 1975, p. 591 (pl. 11, figs. 19, 20); Lazarus, 1990, p. 713 (pl. 3, figs. 8–12).

Antarctissa "bullet" (Pl. **P1,** figs. 5–8).

Remarks: This is a very small antarctissid with an indistinct cephalis and short thorax; height and width are approximately equal; it has a rough surface of small irregular pores and thorns. The base is always closed. This has a complex and not fully detailed set of internal beams. It is similar to *A. cylindrica* but smaller and shows even less evidence of a distinct cephalis either in outline or in cross-sectional view. There is no obvious apical spine. Some specimens have a furrow in the cephalic region, giving a faintly lobed appearance to the shell. These are few–common in late Miocene sediments of the Antarctic.

Helotholus Jörgensen, 1905.

Helotholus? *haysi,* Lazarus, 1992, p. 797 (pl. 8, figs. 1–17).

Lithomelissa Ehrenberg, 1847.

Lithomelissa stigi Bjørklund, 1976, p. 1125 (pl. 15, figs. 12–17).

Lampromitra Haeckel, 1881.

Lampromitra coronata Haeckel, 1887 group, Lazarus 1992, p. 797.

Theoperidae Haeckel, 1881, emend. Riedel, 1967.

Cycladophora Ehrenberg, 1872b, emend. Lombari and Lazarus, 1988.

Cycladophora bicornis (Popofsky) group Lombari and Lazarus, 1988, pp. 106–114 (pls. 4, 5).

Cycladophora pliocenica (Hays) Lombari and Lazarus, 1988, p. 104; Lazarus, 1990, pp. 715–716 (pl. 4, figs. 6, 7).

Cycladophora spongothorax (Chen) Lombari and Lazarus 1988, p. 122 (pl. 9, figs. 7–12); Lazarus, 1990, pp. 715–716 (pl. 4, figs. 1–3).

Pterocanium Ehrenberg, 1847.

Pterocanium korotnevi (Dogiel), Nigrini, 1970, p. 170 (pl. 3, figs. 10, 11).

Lychnocanium Ehrenberg, 1847.

Lychnocanium grande group Campbell and Clark, 1944, p. 42 (pl. 6, figs. 3–6); Lazarus, 1990, p. 717 (pl. 7, fig. 9).
Remarks: This includes both large specimens with characteristic long flared feet and the smaller form seen in older sediments of the late Miocene.

Eucyrtidium Ehrenberg, 1847.

Eucyrtidium calvertense Martin, 1904, p. 450 (pl. 130, fig. 5); Lazarus, 1990, p. 716 (pl. 6, figs. 4–6).

Eucyrtidium pseudoinflatum Weaver, 1983, pp. 675–676 (pl. 5, figs. 8–9); Lazarus, 1990, p. 716 (pl. 6, figs. 12–14).

Eucyrtidium teuscheri group (Haeckel) Caulet, 1986, pp. 850–851 (pl. 5, figs. 1–8).

Stichocorys Haeckel, 1881.

Stichocorys sp. cf. *peregrina* (Riedel) Sanfilippo and Riedel (1970), p. 451 (pl. 1, fig. 10).

Pterocorythidae Haeckel emend. Moore, 1972.

Anthocyrtidium ehrenbergi? (Stöhr) Nigrini and Caulet, 1988, pp. 345–349 (pl. 1, figs. 3, 4).